Actin polymerization or myosin contraction: two ways to build up cortical tension for symmetry breaking

Kevin Carvalho, Joël Lemière, Fahima Faqir, John Manzi, Laurent Blanchoin, Julie Plastino, Timo Betz, C. Sykes

PHILOSOPHICAL TRANSACTIONS OF THE ROYAL SOCIETY B BIOLOGICAL SCIENCES

Actin polymerization or myosin contraction: two ways to build up cortical tension for symmetry breaking

Kevin Carvalho, Joël Lemière, Fahima Faqir, John Manzi, Laurent Blanchoin, Julie Plastino, Timo Betz and Cécile Sykes

Phil. Trans. R. Soc. B 2013 **368**, 20130005, published 23 September 2013

PHILOSOPHICAL TRANSACTIONS OF THE ROYAL SOCIETY B

rstb.royalsocietypublishing.org

Research

Cite this article: Carvalho K, Lemière J, Faqir F, Manzi J, Blanchoin L, Plastino J, Betz T, Sykes C. 2013 Actin polymerization or myosin contraction: two ways to build up cortical tension for symmetry breaking. Phil Trans R Soc B 368: 20130005.
http://dx.doi.org/10.1098/rstb.2013.0005

One contribution of 17 to a Discussion Meeting Issue 'Cellular polarity: from mechanisms to disease'.

Subject Areas:
biophysics, biochemistry, cellular biology

Keywords:
acto-myosin, cortical tension, symmetry breaking, biomimetic liposome

Author for correspondence:
Cécile Sykes
e-mail: cecile.sykes@curie.fr

Actin polymerization or myosin contraction: two ways to build up cortical tension for symmetry breaking

Kevin Carvalho[1,2,3], Joël Lemière[1,2,3,4], Fahima Faqir[1,2,3], John Manzi[1,2,3], Laurent Blanchoin[5], Julie Plastino[1,2,3], Timo Betz[1,2,3] and Cécile Sykes[1,2,3]

[1]Centre de Recherche, Institut Curie, Paris 75248, France
[2]Centre National de la Recherche Scientifique, UMR 168, Paris 75248, France
[3]UPMC University Paris VI, Paris 75005, France
[4]Université Paris Diderot Sorbonne Paris Cité, VII, Paris 75205, France
[5]Laboratoire de Physiologie Cellulaire Végétale, Institut de Recherches en Technologies et Sciences pour le Vivant, CNRS/CEA/INRA/UJF, Grenoble 38054, France

Cells use complex biochemical pathways to drive shape changes for polarization and movement. One of these pathways is the self-assembly of actin filaments and myosin motors that together produce the forces and tensions that drive cell shape changes. Whereas the role of actin and myosin motors in cell polarization is clear, the exact mechanism of how the cortex, a thin shell of actin that is underneath the plasma membrane, can drive cell shape changes is still an open question. Here, we address this issue using biomimetic systems: the actin cortex is reconstituted on liposome membranes, in an 'outside geometry'. The actin shell is either grown from an activator of actin polymerization immobilized at the membrane by a biotin–streptavidin link, or built by simple adsorption of biotinylated actin filaments to the membrane, in the presence or absence of myosin motors. We show that tension in the actin network can be induced either by active actin polymerization on the membrane via the Arp2/3 complex or by myosin II filament pulling activity. Symmetry breaking and spontaneous polarization occur above a critical tension that opens up a crack in the actin shell. We show that this critical tension is reached by growing branched networks, nucleated by the Arp2/3 complex, in a concentration window of capping protein that limits actin filament growth and by a sufficient number of motors that pull on actin filaments. Our study provides the groundwork to understanding the physical mechanisms at work during polarization prior to cell shape modifications.

1. Introduction

In various tissues, for example epithelia, or during vertebrate development, cells are perfectly organized in a polar manner through complex mechanisms that involve biochemical reactions, self-assembly of proteins into scaffolding architectures, and mechanical tension build-up [1]. In the last decade, considerable progress has been made in the identification of the necessary proteins involved in cytoskeletal rearrangements and the establishment of polarity and motility. As a result, it is now possible to reproduce typical phenotypes *in vitro* using these basic elements and to address in detail the different mechanisms involved in polarity establishment. The actin cytoskeleton, together with myosin II, is a crucial player for cellular force production and polarization [2]. These molecular engines drive polarization by actin polymerization and myosin contraction, and their spatial distribution and how they build up tension are key phenomena driving polarization and motility [3,4]. The cell cortex, consisting of a micrometre-thick actin shell underneath the plasma membrane [5], plays a crucial role in ensuring and controlling cellular tension [6,7]. Nucleation of such networks is triggered by biochemical mechanisms, one of them involving the Arp2/3 complex [8]. This complex is activated by proteins from the WASP (Wiskott–Aldrich syndrome protein) family at the membrane where a branched and entangled network emerges [9–11].

Royal Society Publishing
Informing the science of the future

We use biomimetic actin cortices linked to the outside of liposome membranes to address how spherical membranes and cortices that are initially symmetrical can change their shape and polarize. We show that when actin is polymerized at the membrane through the Arp2/3 complex branching mechanism, a stress builds up around the liposome that first relaxes before sustained actin polymerization can propel the liposome into directional movement, reminiscent of the onset of bead motility [11]. Similarly, membrane-attached actin filaments or branched actin networks tightened up by myosin motor activity eventually build up a tension that can relax by local breakage of the network, leading to a polarized actin network. Altogether, our results show that cortical tension around a cell-sized liposome can be generated by distinct mechanisms, all able to induce a spontaneous polarization of actin networks via symmetry breaking. In cells, analogous tension release could modify the distribution of the cytoskeleton and initiate directionality in cells.

2. Material and methods

(a) Reagents

Chemicals are purchased from Sigma Aldrich (St Louis, MO, USA) unless specified otherwise. L-α-Phosphatidylcholine (EPC) and 1,2-distearoyl-sn-glycero-3-phosphoethanolamine-*N*-[biotinyl polyethylene glycol 2000] (biotinylated lipids) and 1,2-dioleoyl-sn-glycero-3-phosphocholine are purchased from Avanti polar lipids (Alabaster, AL, USA).

(b) Proteins

(i) Actin

Actin and biotinylated actin are purchased from Cytoskeleton (Denver, CO, USA) and used with no further purification. Fluorescent Alexa-488 actin is obtained from Molecular Probes. Monomeric actin containing 10 or 20% of labelled Alexa-488 actin and 0.25% of biotinylated actin is diluted in G-Buffer (2 mM Tris, 0.2 mM $CaCl_2$, 0.2 mM dithiothreitol (DTT) at pH 8.0).

(ii) Profilin

Wild-type human profilin in pMW expression vector is transformed into Rosetta 2(DE3) pLysS and expressed in 2 l of LB plus antibiotics overnight at 30°C with 1 mM isopropyl thiogalactopyranoside (IPTG). Cells are lysed and sonicated in 50 mM Tris-Cl pH 7.5, 50 mM sucrose, 10 mM EDTA, 5 mM DTT, 1 mM phenylmethanesulfonylfluoride (PMSF), 2 M urea and complete EDTA-free protease inhibitor cocktail (Roche), then centrifuged at 100 000*g* for 1 h. Supernatants are collected and bound to DEAE-52 cellulose beads for 1 h. Flow through containing profilin is dialyzed against 20 mM Tris-Cl pH 8.0, 20 mM KCl, 1 mM EDTA and centrifuged for 20 min at 100 000*g*. Supernatants are filtered through a 0.2 µm filter and purified by size exclusion over a HiPrep 16/60 Sephacryl S-200 HR column in the dialysis buffer. Profilin is collected and again purified over the Superdex 75 column in the same buffer. Profilin is stored at 4°C.

(iii) His-pWA–streptavidin (S-pVCA)

The In-Fusion (Clontech) cloning method is used to attach human pVCA (verprolin homology central and acidic domain), also called pWA and used in Achard *et al.* [10] and Kawska *et al.* [11], to streptavidin and insert it into pET29 linearized by NcoI/NotI digestion. pVCA is amplified from plasmid pGEX4T1-GST-pWA-His via PCR. The streptavidin gene was a gift of Ahmed El Marjou (Institut Curie). A GSG linker (ggatccgga) is introduced between the pVCA and streptavidin proteins. The resulting pWA–streptavidin is then amplified from the plasmid using a forward oligo that introduces an 8His tag followed by a glycine linker on the 5′ end of the construct and ligated into pET28b(+) via NcoI/NotI digestion. For clone selection, the ligation reaction is transformed into HB101B cells (Invitrogen) to reduce recombination events which pose a problem in this cloning. The construct is transformed into Rosetta 2(DE3) pLysS (Novagen) and expressed in 2 l of LB plus antibiotics, overnight at 20°C with 1 mM IPTG. Cells are lysed and sonicated in 20 mM Tris pH 8.0, 200 mM NaCl, 40 mM imidazole pH 8.0, 0.1% Triton X-100, 1 mM DTT and complete EDTA-free protease inhibitor cocktail (Roche), then bound to Ni-sepharose high performance beads (GE Healthcare). Unbound proteins are washed away with 20 mM Tris pH 8.0, 200 mM NaCl, 40 mM imidazole pH 8.0, 1 mM DTT, and bound proteins are eluted in the same buffer containing 300 mM imidazole. Proteins are further purified over the Superdex 200 10/300GL column (GE Healthcare) in 20 mM Tris pH 8.0, 200 mM NaCl, 0.5 mM ETDA, 1 mM DTT. Pure protein is dialysed into the same buffer containing 5% glycerol and stored at −80°C. The activity of S-pVCA is checked by a pyrene assay [12] in the presence of the Arp2/3 complex, profilin and actin, and found to be slightly more active than His-pWA (or p-VCA).

(iv) Other proteins

Bovine Arp2/3 complex is purchased from Cytoskeleton and used with no further purification. Mouse capping protein (CP; α_1/β_2) is purified as previously described [13]. Myosin II is purified from rabbit skeletal muscle, and fluorescent myosin II is prepared as previously described [14]. The working buffer contains 25 mM imidazole, 50 mM KCl, 70 mM sucrose, 1 mM Tris, 2 mM $MgCl_2$, 1 mM ATP, 0.1 mM DTT, 0.02 mg ml^{-1} casein, adjusted to pH 7.4. All proteins are mixed in the working buffer and myosin II forms minifilaments of approximately 0.7 µm length with about 100 motors [14].

(c) Liposome and actin cortex formation and observations

Liposomes are electroformed [15]. Briefly, 20 µl of a mixture of EPC lipids and 0.1% biotinylated lipids with a concentration of 2.5 mg ml^{-1} in chloroform/methanol 5 : 3 (v : v) are spread on indium tin oxide (ITO)-coated plates under vacuum for 2 h. A chamber is formed using the ITO plates (their conductive sides facing each other) filled with the formation buffer (200 mM sucrose, 2 mM Tris adjusted at pH 7.4) and sealed with haematocrit paste (Vitrex Medical, Denmark). Liposomes are formed by applying an alternate current voltage (10 Hz) for 75 min. Note that osmolarities of the formation buffer and the working buffer are matched. The actin cortex is obtained either by (i) polymerizing the branched actin network directly from the surface through an activator of actin polymerization linked to the membrane or (ii) linking actin filaments directly to the liposome membrane. To induce actin polymerization (i), liposomes are first incubated in 0.1 µM S-pVCA solution and are then diluted 10 times in a mix containing 1 µM monomeric actin containing 10% fluorescent actin monomers and no biotinylated actin monomers, 3 µM profilin, 50 nM of the Arp2/3 complex and various quantities of CP. Actin filaments (F-actin) for linking directly to the membrane in procedure (ii) are obtained by polymerizing, during 1 h, 1 µM or 3 µM of G-actin containing 10% fluorescently labelled G-actin and 0.25% biotinylated G-actin in the presence of phalloidin (1 : 1 ratio with actin monomer concentration). In parallel, liposomes made with biotinylated lipids are incubated with 160 nM of streptavidin for 15 min. To induce F-actin binding on the membrane, biotinylated F-actin is diluted to 0.1 µM and mixed with streptavidin-coated liposomes for 15 min. The mix is diluted 10-fold and flowed into an observation chamber made by heating two Parafilm

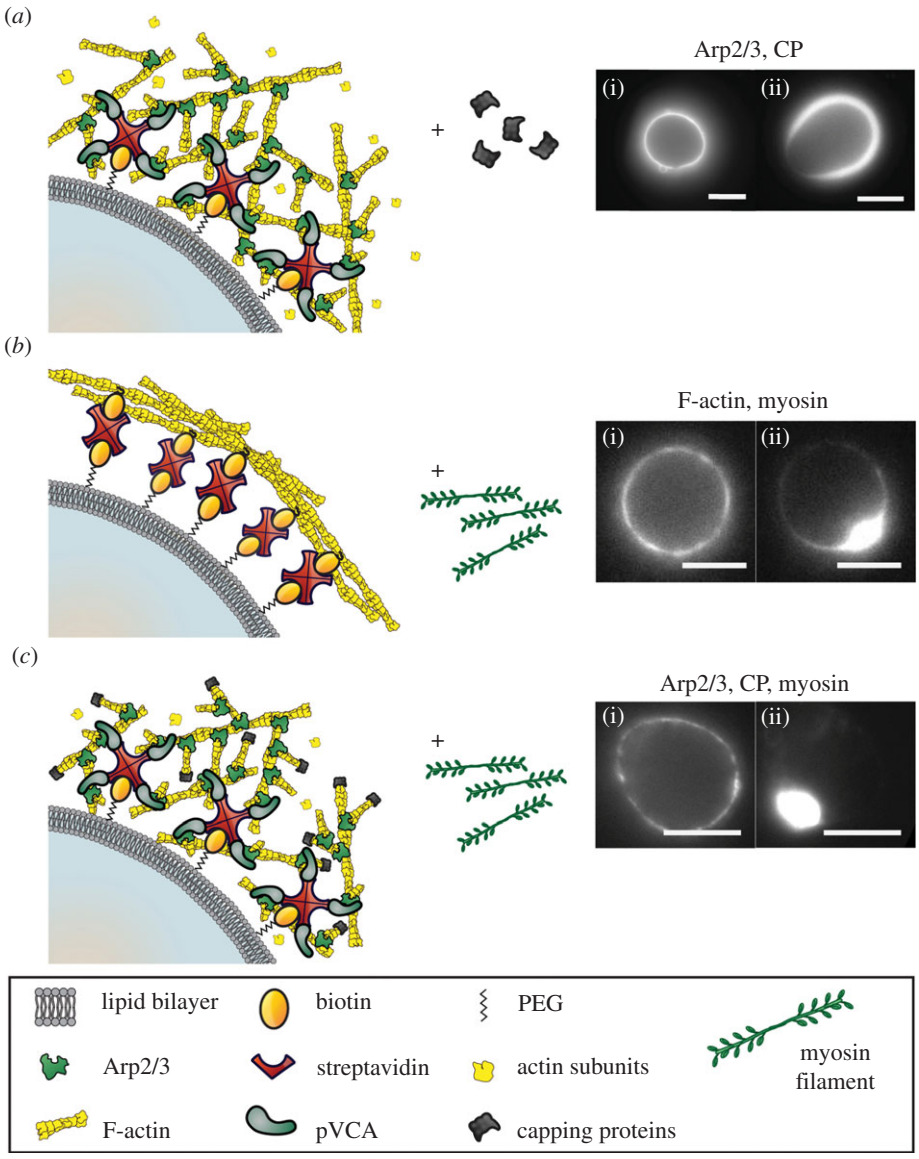

Figure 1. Stress build-up and symmetry breaking of an actin network on a liposome membrane. Left: three different experimental situations schematized (proteins not to scale). Right: epifluorescence images of fluorescently labelled actin. (*a*) Actin filaments are nucleated from a liposome membrane by 50 nM of the Arp2/3 complex in the absence (i) or in the presence (ii) of 20 nM of CP. (*b*) Fluorescently labelled actin filaments (F-actin) are linked to the liposome membrane by a biotin–streptavidin link in the absence (i) or in the presence (ii) of 20 nM myosin II filaments. (*c*) Actin filaments nucleated from a liposome membrane by 50 nM of the Arp2/3 complex in the presence of 10 nM of CP and in the absence (i) or in the presence (ii) of 20 nM of myosin II filaments. Scale bars, 5 µm.

stripes (as spacers) between two coverslips. Five minutes later, after checking that actin-decorated liposomes are observed, myosin II minifilaments are flowed into the chamber. Epifluorescence and phase contrast microscopy are performed using an IX70 Olympus inverted microscope with a 100× or a 60× oil-immersion objective. Spinning disk confocal microscopy is performed on a Nikon Eclipse T1 microscope with an Andor Evolution scan head equipped with an Andor Neo sCMOS camera and using a 60× water immersion objective (NA = 1.20). Imaris ×64 7.4.0 is used for three-dimensional reconstructions with no deconvolution. Randomly chosen liposomes are imaged over time. Intensity profiles are made using Image J. The radius of liposomes carrying actin is measured as the average distance between the liposome centre and the point of maximal intensity.

3. Results

In order to mimic in a controlled fashion the actin cortex next to the plasma membrane, cell-sized liposomes are covered with actin networks to form a shell. We use an 'outside' geometry that allows a perfect control of protein composition and concentrations, although the 'inside' geometry is possible but limited in protein concentration changes that we can apply [16,17]. Two different actin networks are reconstituted at the surface of the liposome membrane that contains biotinylated lipids (figure 1). An actively polymerizing branched network is formed by recruiting the Arp2/3 complex at the membrane via the VCA domain of WASP, which is linked by a streptavidin tag to the membrane, and in the presence of CP (figure 1*a*,*c*). A randomly distributed, non-growing actin filament network is linked to the liposome surface through streptavidin–biotin linkers (figure 1*b*). We observe that each of these conditions leads to the formation of a homogeneous actin shell (i) that becomes heterogeneous (ii) when CP (figure 1*a*) or myosin (figure 1*b*,*c*) is added. When actin continuously polymerizes at the liposome surface (figure 1*a*), stress is accumulated in the network [18]. As described previously, the liposome is able to move after symmetry has broken, and actin appears thinner at the front of the moving liposome, whereas the actin network appears thicker at the rear [19–21]. During movement, actin continues

to polymerize and thus propels the liposome forward through continuous squeezing forces [22,23]. In the two other cases, either actin filaments are already polymerized (figure 1*b*), or the branched network is already formed (figure 1*c*). In these cases, the reorganization of the actin shell relies entirely on the effect of myosin motors, and after contraction has occurred the system does not further evolve. In all cases presented here, symmetry breaks either through actin polymerization or myosin motor forces. Although both mechanisms are at work simultaneously in cells [24], our simplified system allows us to study them separately.

(a) Polymerization of actin induces symmetry breaking depending on capping protein concentration

In order to recruit and activate the Arp2/3 complex to nucleate actin polymerization at the membrane, we use a fragment of WASP, S-pVCA, that is designed to stick to the biotinylated lipids composing the liposome membrane (see Material and methods). Liposomes incubated with S-pVCA are diluted in the working buffer containing the Arp2/3 complex, profilin and CP (see Material and methods) as for branched actin networks grown from polystyrene beads [10,11]. The presence of profilin allows actin branch nucleation to occur mainly at the liposome surface decorated with the S-pVCA and prevents actin filament polymerization in the bulk. Concentrations of the Arp2/3 complex and profilin are kept constant, whereas CP concentration is varied from 0 to 50 nM. In the absence of CP, it has been shown in similar conditions with other systems that actin filaments nucleate by branching at the surface and grow with their barbed ends directed away from the membrane surface [10,11]. In our case, the actin cloud remains homogeneous and symmetry breaking is never observed, because the polymerization force is only used for elongating the filaments homogeneously away from the liposome membrane against the viscous solution (figure 2*a* left, black symbols). When CP is added, the elongation of branched filaments is limited by capping, as can be seen by the decrease of the fluorescence intensity profile outside the liposome that is sharper in the presence of CP than when CP is absent (compare figure 2*a*,*b*). As polymerization continues at the sites of immobilized S-pVCA at the liposome surface, capped branches get pushed away from the surface by the actin filament trees that entangle in a cohesive network [11,25]. At first, the actin network remains homogeneous during this process until liposomes deform and symmetry breaking occurs (elongated shape of liposomes in figure 2*b*,*c*), similar to what is observed around beads [11,18]. Indeed, the cohesive network in the spherical geometry of the liposome is deformed (stretched) during growth and, as a result, a tangential stress develops within the actin shell. This stress is highest on the outside layer and lowest at the liposome surface, where in fact its value is zero because new polymerization occurs at the surface. This stress (a force per unit surface) within the actin shell results in a global tension (a force per unit length) of the actin shell, which is obtained by the integral of the tangential stress over the actin shell thickness. As actin polymerization continues, the tangential stress, and therefore the tension of the shell, increases, until it overcomes a critical stress (or tension) that generates shell breakage. On beads, this tension was clearly demonstrated by photodamaging the actin shell, which consequently broke open by a tension-release mechanism [18]. Note that shell breakage is followed by the expulsion of the liposome from the growing actin shell, creating a propelling comet tail and actin-based motility owing to pushing forces through squeezing stresses, a phenomenon that has been thoroughly studied elsewhere [18,23]. The state of the actin shell is reported on the graphs in figure 2 as a function of the time of observation for different liposome sizes. The separation of the red symbols (symmetry is broken) from the black symbols (symmetry is not broken) represents the symmetry breaking time that is observed to increase in a linear fashion with liposome radius (dashed lines figure 2*b*,*c*), in agreement with previous studies on hard spheres and with a comparable proportionality coefficient of about 0.25–1.5 min μm^{-1} depending on CP concentration [26]. However, in contrast to rigid polystyrene spheres, liposomes allow for the observation of active deformation owing to stress accumulation that typically occurs before the symmetry breaks (figure 2*c*). In the presence of 50 nM CP, actin subnetworks emerging from the Arp2/3 complex are not sufficiently entangled to build up enough tension for symmetry breaking (figure 2*d*). These observations confirm a previous study on hard beads [11] showing that symmetry breaking happens in a concentration window of CP (figure 2*b*,*c*). Altogether, our results show that when branched actin networks are nucleated at a liposome membrane, stress can build up, and generate tension and deformation of the liposome followed by breakage of the shell. This happens if branches are limited in their growth, but long enough to entangle [11].

(b) A preformed actin filament network shell can break symmetry in the presence of myosin motors

In order to investigate how polymerization forces differ from acto-myosin contraction forces, we turn to a non-polymerizing actin network in the presence of myosin motors. Preformed actin filaments with an average length of 4 μm measured by electron microscopy [27] are linked to the membrane via a streptavidin–biotin bond (figure 1*b*) and each actin filament carries an average of four biotins (0.25% biotin–actin label). In the absence of myosin motors, such a system does not build up an intrinsic stress, as we never observe any liposome deformation and symmetry breaking. Upon myosin II injection in the chamber, the shell breaks open (figure 3*a*). The time at which the symmetry breaking happens does not depend on the liposome radius (figure 3*b*). The volume of the liposomes is observed by filling them with 0.9 μM of sulforhodamine B, a red fluorescent dye (figure 3*c*). The volume of the liposome (red) and the actin shell (green) can be observed simultaneously by spinning disk confocal microscopy (figure 3*c*,*d*). Symmetry breaks in a 'peeling' process, where the actin shell first deforms the liposome then contracts on one side. To highlight where the deformation occurs around the liposome, we subtract two images of the equatorial section of the liposome volume (red channel, before and after deformation) and take the absolute value of the subtracted intensity. This treatment results in a map of the liposome contour (10-pixel thickness) deformations (figure 3*d*). If the liposome is not deformed then the variation of intensity is low, whereas under liposome deformation the variation of intensity is high (figure 3*d*, lower panel). The time at which the peeling contraction starts depends on myosin concentration and decreases from about 17 min to 3 min for myosin concentrations of 2 and 200 nM, respectively [27]. Strikingly, the duration of contraction and the speed of

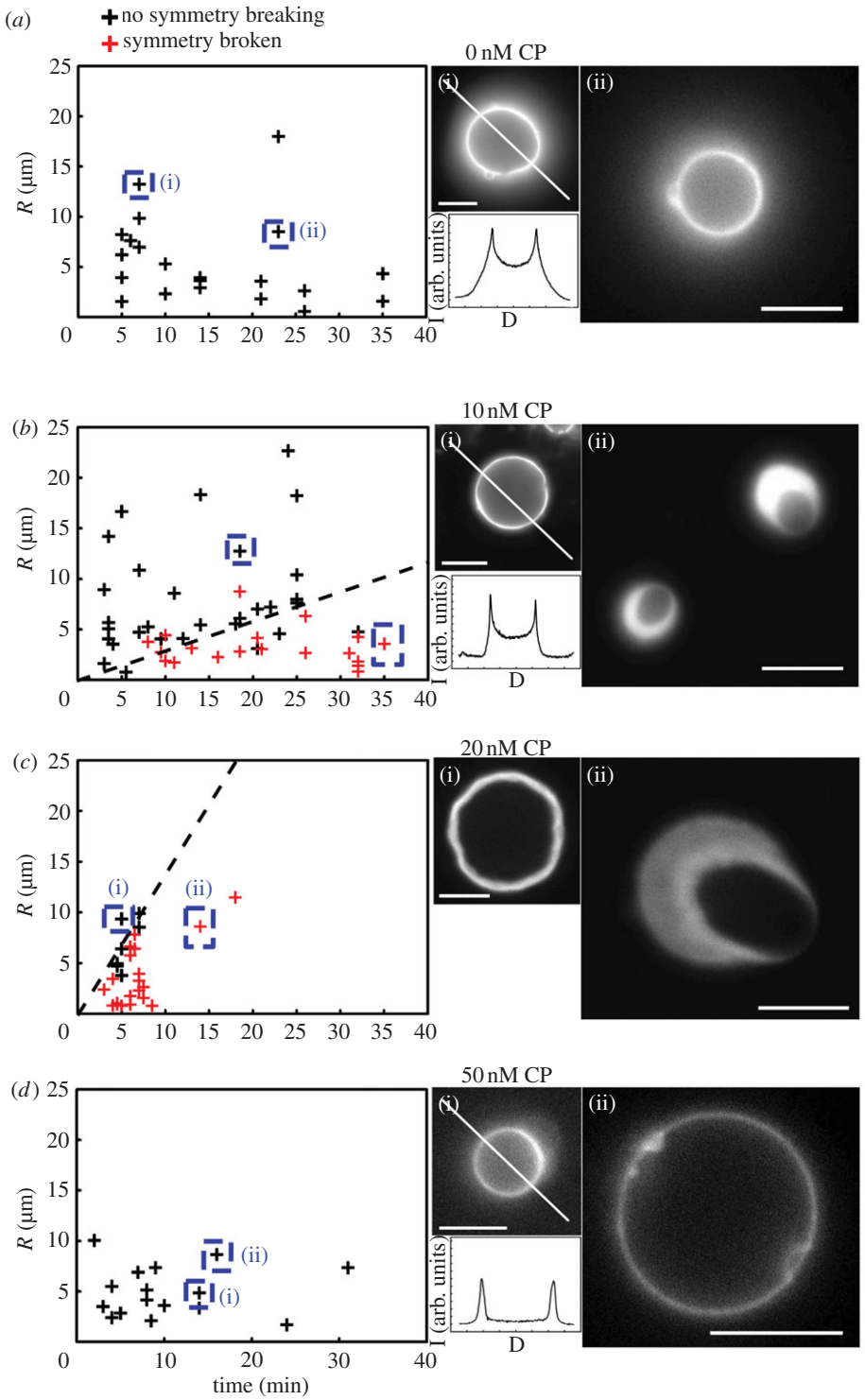

Figure 2. Polymerization of a branched actin network around cell-sized liposomes membranes can induce stress build-up and symmetry breaking. (*a*,*b*,*d*) Epi-fluorescence images (i) and (ii). (*c*) Spinning disk confocal microscopy images (i) and (ii). (*a*–*d*) Time zero corresponds to the start of the polymerization of 1 µM actin in the presence of 50 nM Arp2/3, 3 µM profilin and the indicated concentration of CP. The sizes of the observed liposomes over time are plotted for each concentration of CP as red symbols if the symmetry has already broken or black symbols if the shell appears homogeneous. The black dashed line indicates the border between broken or not broken actin shells. The symbols surrounded by a blue dashed rectangle are the liposomes represented in (i) and (ii) as examples of non-symmetry broken and symmetry broken liposomes. Below (i) is the corresponding intensity profile over the distance D along the white line in (i), except for the spinning disk images in (*c*). Scale bars, 10 µm. Between 20 and 50 liposomes were observed in each condition.

retraction (peeling) are independent of myosin concentration [27] and of the order of 1 min for the duration and about $14 + 6\ \mu m\ min^{-1}$ for the retraction speed in a 2–200 nM myosin concentration range (figure 3*a*,*c*). The constant peeling duration when myosin concentration is varied indicates that the peeling mechanism is independent of myosin activity and indicates a purely elastic relaxation mechanism. However, the time at which peeling starts does decrease when myosin concentration is increased, indicating that a sufficient quantity of myosin motors needs to be present for peeling to start.

(c) Contractility of a branched actin network in the presence of myosin

In order to go one step further in the reconstruction of the contractility of a cell cortex, we combine the two approaches

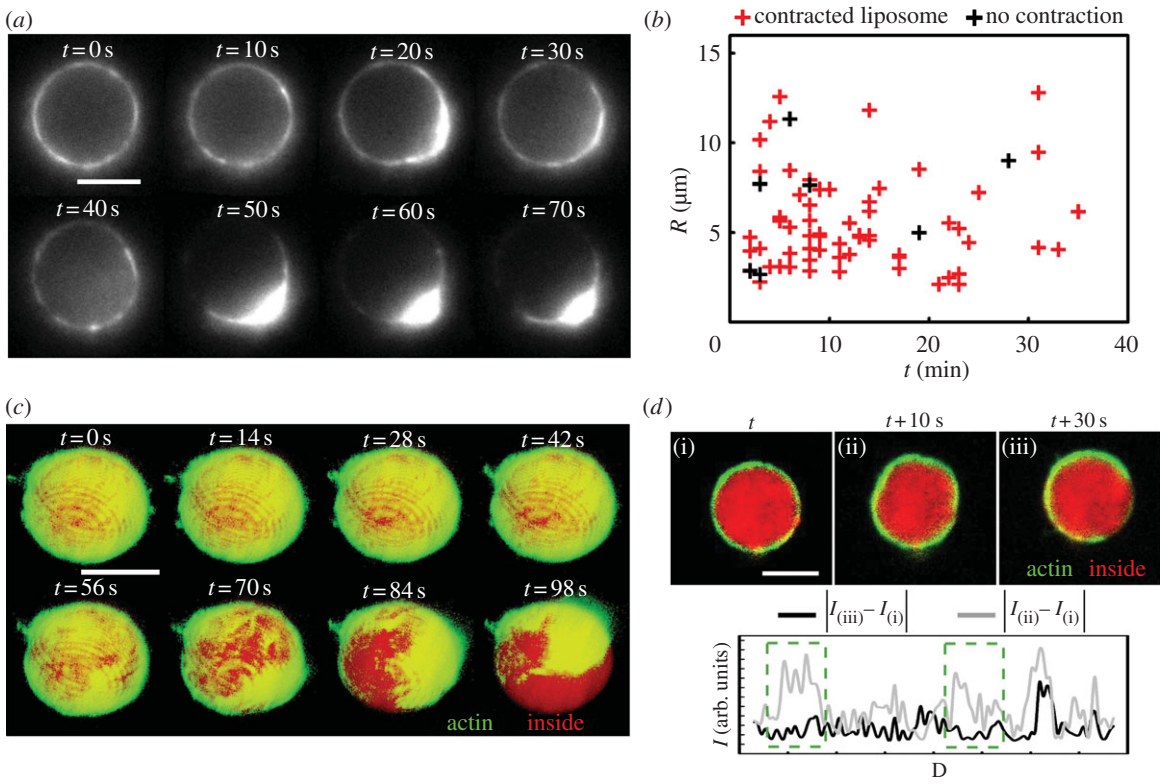

Figure 3. Acto-myosin contraction of fluorescent actin filaments organized into a shell. Time-lapse images in epifluorescence (*a*) and spinning confocal microscopy (*c*,*d*). Time (*t*) indicated in white. (*a*) Contraction of an actin shell after injection of 20 nM myosin II minifilaments in the observation chamber. (*b*) Size of contracted and uncontracted liposomes over time; time zero corresponds to the injection of myosin II minifilaments. Symbols mark the state, contracted in red or not in black, of the liposome (78 liposomes). (*c*) Time lapse of three-dimensional reconstruction with actin (green) and inside solution (red); time zero corresponds to the start of the contraction. (*d*) Time lapse of a spinning disk confocal slice at the equatorial plane of the liposome with actin (green) and inside solution (red): (i) before contraction, (ii) just before actin distribution becomes heterogeneous, and (iii) when the actin network ruptures. Below each image is the absolute value of the intensity difference in the red channel over the distance D along the contour of the liposome: black curve, difference of (iii) and (i); grey curve, difference of (ii) and (i). Green dotted boxes show the regions of high variation in intensity corresponding to the most deformed regions. Scale bar, 5 μm.

described above to produce a branched actin network contracted by myosin motors. This is physiologically relevant as the Arp2/3 complex has been shown to participate in the construction of the acto-myosin network in cells [8] and its properties have been studied *in vitro* [28]. We choose conditions where the stress owing to actin polymerization and branching is not high enough to break the symmetry (0 and 50 nM CP; figure 2*a*,*d*) or where the symmetry breaks later than the time at which we inject myosin (10 nM CP; figure 2*b*). We want to address here if and how a branched network is able to contract in the presence of myosin II motors and, in particular, the role of filament length. For that, we vary the concentration of CP when forming the actin shell. In the absence of CP, when myosin motors are added, no contraction happens (figure 4*a*). In the absence of CP, there are two kinds of coexisting networks: the branched network at the vicinity of the membrane where the Arp2/3 complex is activated by S-pVCA, and long parallel filaments coming out of the branched network and elongating with their barbed ends far away from the membrane [10]. As myosin motors move toward the barbed end and are unable to contract parallel actin filaments, they may not reach the branched filaments that lie on the two-dimensional plane of the membrane in our 20 min observation window, consistent with observations on patterned substrates [28]. In the presence of 10 nM CP, contraction is observed and the actin shell is peeled away similar to the situation of figure 3 and aggregates together with myosin motors on one side of the liposome (figure 4*b*). Increasing the CP concentration to 50 nM leads to the loss of actin rearrangement even if myosin is observed to interact with the actin network (figure 4*c*). In this case, there is no contraction and no symmetry breaking as actin subnetworks form a loosely entangled actin network unable to sustain tension and to accumulate stress. Myosin is generally thought to work on linear filaments, but here we show clearly that branched networks, nucleated by 50 nM of Arp2/3 complex, contract in the presence of myosin II minifilaments in a CP concentration window of 10–20 nM (figure 4*d*).

4. Discussion

Initiation of cell polarization is difficult to study in cells because it is a complex, multi-scale phenomenon downstream of signalling events and leading to cell-scale deformation. Our controlled system gives an alternative way of studying fundamental biochemical and physical mechanisms triggering contraction and polarization induced by myosin II and actin polymerization dynamics.

(a) Stress build-up can arise from different mechanisms

We show that tension can build up around a liposome, generated either by pure actin polymerization stresses or by pulling forces of myosin motors. The tension increase in the network is due to either actin dynamics only or the action of molecular motors that slide actin filaments relative to each other, creating strain that results in stress. In both cases, we observe that the liposome deforms prior to symmetry breaking (figures 2*c* and 3*d*). This indicates that even though the intrinsic tension

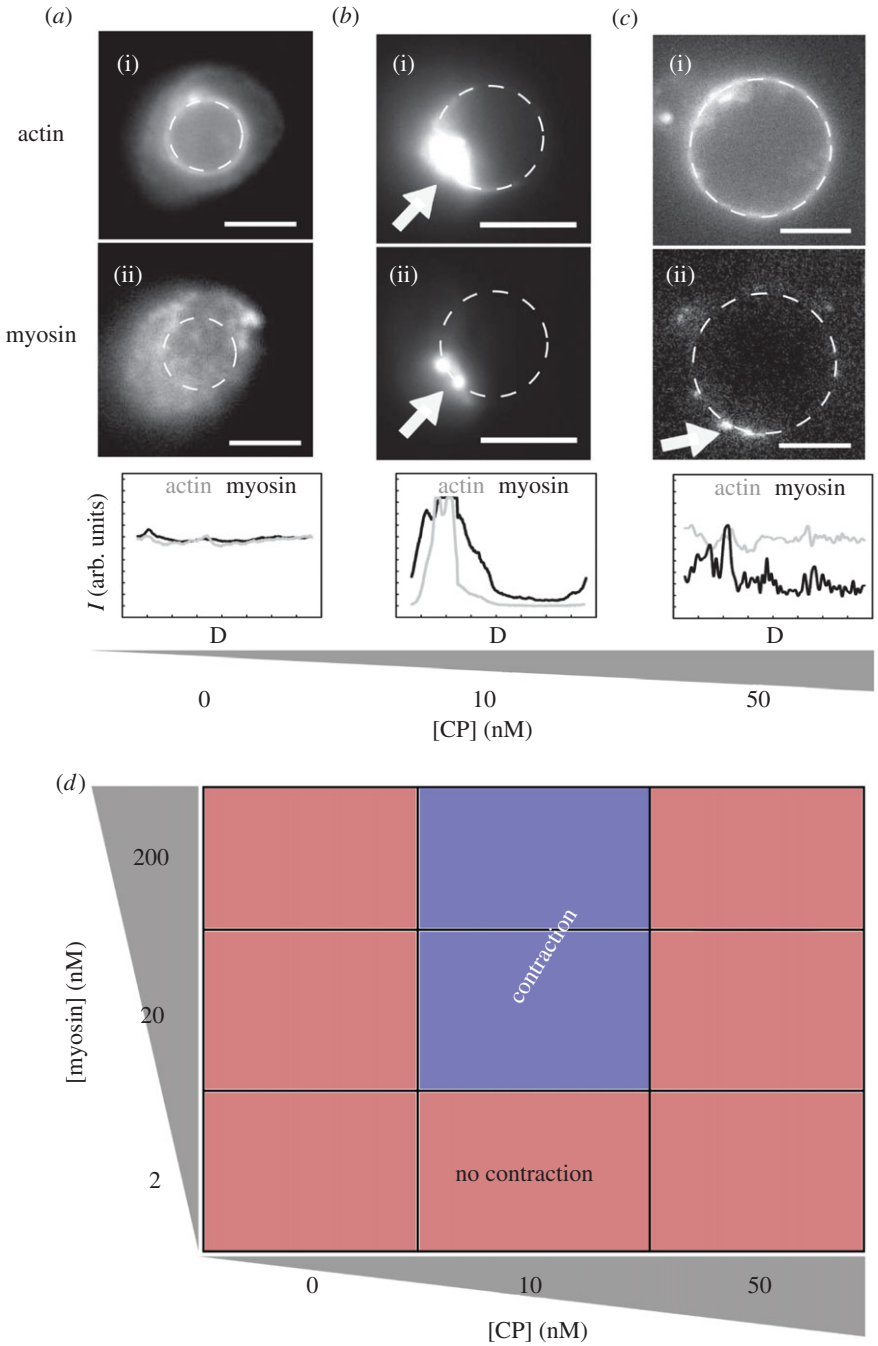

Figure 4. Contraction of branched actin networks by myosin II. (*a–c*) Epifluorescence images of (i) actin and (ii) myosin II, for different CP concentrations as indicated. The position of the liposome is given by the white dashed line, and the corresponding intensity profiles over the distance D along the contour for actin channel and myosin channel are given below the images (actin in grey, myosin in black). (*d*) Diagram of contraction as a function of myosin and CP concentration. Scale bar, 5 μm.

is not yet high enough to rupture the network and trigger polarization, it can deform the membrane.

We are able here to distinguish the tension induced by actin polymerization from the tension induced by myosin motors. When actin polymerizes, the symmetry breaking time depends on the size of the liposome (figure 2) and the velocity of polymerization [29], whereas it does not depend on liposome size when the tension is myosin induced (figure 3). In myosin-contracting shells, the time for symmetry to break is governed by the number of myosin motors able to interact with the actin network (figures 2*b* and 3*b*).

Polymerization forces generate a tangential stress in the actin network that is maximal on the outer layer of the shell. The integral of the tangential stress over the thickness of the actin gel results in a tension. When this tension is higher than a threshold for rupture of the actin network, the shell breaks and relaxes tension. This threshold tension depends on the radius of the liposome and decreases when the liposome radius increases, explaining why larger liposomes break symmetry more slowly (figure 2*b*,*c*). Likewise, myosin contraction forces generate tension in the actin shell that is able to break when the threshold in myosin motor number, and therefore tension, is exceeded. In both cases, polymerization forces or contractile forces by myosin motors, this threshold tension is increased in the presence of cross-linkers that reinforce the actin network making it more difficult to break [18,27]. In the case of a branched actin network put under tension by myosin motors, the formation of a hole or a crack may be facilitated by depolymerization under contraction, a phenomenon shown

in vitro in a different geometry [28] and shown in cells where motors disassemble the actin network at the rear of motile cells or at the back of the lamellipodium [29]. Once a hole has opened in the actin shell, the network retracts through an elastic relaxation, like the release of a stretched rubber band. In the case of polymerization forces, the continuously growing actin network can propel the liposome by squeezing forces as the network is continuously generating stresses [19,21,22]. When myosin-generated tension has relaxed, no further contraction or movement is observed in the case of figures 3 and 4.

In all cases, the morphology of the network and the lengths of filaments or branches are crucial to achieve contraction (figure 4). Indeed, without CP, the actin filaments are long and organized in a parallel fashion away from the surface. In this case, the polarity of actin filaments is such that myosin filaments actively move outward, which prevents the motor from entering into the branched network at the vicinity of the membrane (figure 4*a*). In the presence of CP, myosin is able to contract the branched network. It is important to note that the concentration window of CP in which we obtain myosin-induced contraction is similar to the one where symmetry breaking is observed with polymerizing networks (figures 2 and 4) [11].

5. Conclusion

We reproduce an actin cortex around a liposome membrane and show that intrinsic tension build-up arises from two distinct mechanisms: active polymerization and myosin II motor activity. Spontaneous polarization of the system is due to accumulated stress that reaches the critical stress needed to break the network. In the case of branched actin networks either with or without myosin, the main regulator of polarization is CP, which regulates the length of actin filaments. Extrapolating our work to the context of the cell, forces in cells can be generated by two different mechanisms, based either on pure actin polymerization or on pure myosin contraction. The density of the actin network and especially the length of the actin filaments in the network might be a crucial element for controlling contraction and polarization. Note that cortical flows in cells have both polymerization and motor mechanisms at work, as actin constantly polymerizes at the cell membrane, whereas acto-myosin contraction squeezes the cortex and presumably enhances actin disassembly for actin turn-over. Our work paves the way for a reconstitution of both active systems at the same membrane.

Acknowledgements. We thank G.H. Koenderink and F.C. Tsai for teaching us the purification of myosin II minifilaments. We acknowledge Dr Agnieszka Kawska at IlluScientia.com for the graphical representation of figure 1.

Funding statement. This work was supported by the French ANR grant nos. ANR 09BLAN0283, ANR 12BSV5001401 and ANR-11-JSV5-0002, and by the Fondation pour la Recherche Médicale (FRM) grant no. DEQ20120323737. K.C. was supported by a post doc fellowship from the Association pour la Recherche contre le Cancer (ARC) and J.L. by doctoral fellowship from AXA research fund.

References

1. Levayer R, Lecuit T. 2012 Biomechanical regulation of contractility: spatial control and dynamics. *Trends Cell Biol.* **22**, 61–81. (doi:10.1016/j.tcb.2011.10.001)
2. Salbreux G, Charras G, Paluch E. 2012 Actin cortex mechanics and cellular morphogenesis. *Trends Cell Biol.* **22**, 536–545. (doi:10.1016/j.tcb.2012.07.001)
3. Hawkins RJ, Poincloux R, Bénichou O, Piel M, Chavrier P, Voituriez R. 2011 Spontaneous contractility-mediated cortical flow generates cell migration in three-dimensional environments. *Biophys. J.* **101**, 1041–1045. (doi:10.1016/j.bpj.2011.07.038)
4. Sedzinski J, Biro M, Oswald A, Tinevez J-Y, Salbreux G, Paluch E. 2011 Polar actomyosin contractility destabilizes the position of the cytokinetic furrow. *Nature* **476**, 462–466. (doi:10.1038/nature10286)
5. Morone N, Fujiwara T, Murase K, Kasai RS, Ike H, Yuasa S, Usukura J, Kusumi A. 2006 Three-dimensional reconstruction of the membrane skeleton at the plasma membrane interface by electron tomography. *J. Cell Biol.* **174**, 851–862. (doi:10.1083/jcb.200606007)
6. Tinevez J-Y, Schulze U, Salbreux G, Roensch J, Joanny J-F, Paluch E. 2009 Role of cortical tension in bleb growth. *Proc. Natl Acad. Sci. USA* **106**, 18 581–18 586. (doi:10.1073/pnas.0903353106)
7. Paluch E, Piel M, Prost J, Bornens M, Sykes C. 2005 Cortical actomyosin breakage triggers shape oscillations in cells and cell fragments. *Biophys. J.* **89**, 724–733. (doi:10.1529/biophysj.105.060590)
8. Fritzsche M, Lewalle A, Duke T, Kruse K, Charras G. 2013 Analysis of turnover dynamics of the submembranous actin cortex. *Mol. Biol. Cell.* **24**, 757–767. (doi:10.1091/mbc.E12-06-0485)
9. Machesky LM, Mullins RD, Higgs HN, Kaiser DA, Blanchoin L, May RC, Hall ME, Pollard TD. 1999 Scar, a WASp-related protein, activates nucleation of actin filaments by the Arp2/3 complex. *Proc. Natl Acad. Sci. USA* **96**, 3739–3744. (doi:10.1073/pnas.96.7.3739)
10. Achard V, Martiel J-L, Michelot A, Guérin C, Reymann A-C, Blanchoin L, Boujemaa-Paterski R. 2010 A primer-based mechanism underlies branched actin filament network formation and motility. *Curr. Biol.* **20**, 423–428. (doi:10.1016/j.cub.2009.12.056)
11. Kawska A, Carvalho K, Manzi J, Boujemaa-Paterski R, Blanchoin L, Martiel J-L, Sykes C. 2012 How actin network dynamics control the onset of actin-based motility. *Proc. Natl Acad. Sci. USA* **109**, 14 440–14 445. (doi:10.1073/pnas.1117096109)
12. Cooper JA, Walker SB, Pollard TD. 1983 Pyrene actin: documentation of the validity of a sensitive assay for actin polymerization. *J. Muscle Res. Cell. Motil.* **4**, 253–262. (doi:10.1007/BF00712034)
13. Soeno Y, Abe H, Kimura S, Maruyama K, Obinata T. 1998 Generation of functional beta-actinin (CapZ) in an *E. coli* expression system. *J. Muscle Res. Cell. Motil.* **19**, 639–646. (doi:10.1023/A:1005329114263)
14. Silva MSE, Depken M, Stuhrmann B, Korsten M, Mackintosh FC, Koenderink GH. 2011 Active multistage coarsening of actin networks driven by myosin motors. *Proc. Natl Acad. Sci. USA* **108**, 9408–9413. (doi:10.1073/pnas.1016616108)
15. Angelova M, Dimitrov D. 1986 Liposome electroformation. *Faraday Discuss.* **81**, 303. (doi:10.1039/dc9868100303)
16. Pontani L-L, Van der Gucht J, Salbreux G, Heuvingh J, Joanny J-F, Sykes C. 2009 Reconstitution of an actin cortex inside a liposome. *Biophys. J.* **96**, 192–198. (doi:10.1016/j.bpj.2008.09.029)
17. Tsai F-C, Stuhrmann B, Koenderink GH. 2011 Encapsulation of active cytoskeletal protein networks in cell-sized liposomes. *Langmuir* **27**, 10 061–10 071. (doi:10.1021/la201604z)
18. Van der Gucht J, Paluch E, Plastino J, Sykes C. 2005 Stress release drives symmetry breaking for actin-based movement. *Proc. Natl Acad. Sci. USA* **102**, 7847–7852. (doi:10.1073/pnas.0502121102)
19. Giardini PA, Fletcher DA, Theriot JA. 2003 Compression forces generated by actin comet tails on lipid vesicles. *Proc. Natl Acad. Sci. USA* **100**, 6493–6498. (doi:10.1073/pnas.1031670100)
20. Heuvingh J, Franco M, Chavrier P, Sykes C. 2007 ARF1-mediated actin polymerization produces

movement of artificial vesicles. *Proc. Natl Acad. Sci. USA* **104**, 16 928–16 933. (doi:10.1073/pnas.0704749104)

21. Van Oudenaarden A, Theriot JA. 1999 Cooperative symmetry-breaking by actin polymerization in a model for cell motility. *Nat. Cell Biol.* **1**, 493–499. (doi:10.1038/70281)
22. Boukellal H, Campás O, Joanny J-F, Prost J, Sykes C. 2004 Soft Listeria: actin-based propulsion of liquid drops. *Phys. Rev. E Stat. Nonlin. Soft. Matter Phys.* **69**, 061906. (doi:10.1103/PhysRevE.69.061906)
23. Plastino J, Sykes C. 2005 The actin slingshot. *Curr. Opin. Cell Biol.* **17**, 62–66. (doi:10.1016/j.ceb.2004.12.001)
24. Bray D, White JG. 1988 Cortical flow in animal cells. *Science* **239**, 883–888. (doi:10.1126/science.3277283)
25. Sykes C, Plastino J. 2010 Cell biology: actin filaments up against a wall. *Nature* **464**, 365–366. (doi:10.1038/464365a)
26. Bernheim-Groswasser A, Wiesner S, Golsteyn RM, Carlier M-F, Sykes C. 2002 The dynamics of actin-based motility depend on surface parameters. *Nature* **417**, 308–311. (doi:10.1038/417308a)
27. Carvalho K, Tsai F-C, Lees E, Voituriez R, Koenderink GH, Sykes C. Submitted. Cell sized liposomes reveal how acto-myosin cortical tension drives shape change.
28. Reymann A-C, Boujemaa-Paterski R, Martiel J-L, Guérin C, Cao W, Chin HF, De La Cruz EM, Théry M, Blanchoin L. 2012 Actin network architecture can determine myosin motor activity. *Science* **336**, 1310–1314. (doi:10.1126/science.1221708)
29. Wilson CA *et al*. 2010 Myosin II contributes to cell-scale actin network treadmilling through network disassembly. *Nature* **465**, 373–377. (doi:10.1038/nature08994)